



มหาวิทยาลัยมหิดล
Mahidol University

**1-D forward modeling of transient electromagnetic:
solutions for magnetic field according to ground-dipole source**

Submitted June 2020, in partial fulfillment of the conditions
for the award of the degree **Bachelor of Science in Physics**

Wasinee Rattapasakorn

Advisor

Dr. Puwis Amatyakul

Geophysics Research Group, Department of Physics

Faculty of Science, Mahidol University

June, 2020

Abstract

Long Offset Time-domain Electromagnetic (LOTEM) method is the geophysical method used for hydrocarbon (oil and gas) exploration (Ward, 1987). The LOTEM method consists of a grounded dipole far away from the receivers, injecting time-varying electrical current into the subsurface. Each receiver composes of electrodes for measuring the electric field and air loop for measuring the vertical magnetic field. The distance between the transmitter and receiver site is called offset. The offset is approximately equal to or greater than the exploration depth for the LOTEM method (Strack, 1992). When the explorer injected current into the ground through the transmitter dipole source. Current switching causes the primary magnetic field induction, which will cause subsequent eddy current in the subsurface. After that, the eddy current induced the secondary magnetic field according to Faraday's law, which the currents diffuse in the subsurface is related to the conductivity distribution in the ground. The receivers measure voltage differences between ground in two directions and the vertical magnetic fields. The resistivity contrast of the structure beneath the ground can be obtained by changing the transient curve and the transient time depending on the depth of the structure (Strack et al., 1989).

Forward modeling is a tool for geophysicists that uses numerical methods to compute the geophysical response from the assumed initial structure (Christiansen et al, 2009; 2015). The LOTEM method uses the derivative of vertical magnetic intensity, which is derived from the inverse Fourier sine transform of the imaginary part of the vertical magnetic intensity for the forward modeling.

However, if the exploration take place in the urban area, there will be cultural noises from made-made instruments. The strength of the derivative of vertical magnetic intensity measured from air-loop could be less than the level of the cultural noise. To tackle this limitation, the vertical magnetic intensity measured by the fluxgate magnetometer is proposed which proved to have signal strength much greater than the cultural noise (Rochlitz et al., 2018). In order to make use of the proposed vertical magnetic intensity, the 1-D forward modeling is the need to be developed.

Keywords: Transient Electromagnetic, LOTEM method, Magnetic field, Forward modeling

Acknowledgement

The author would like to thank the advisor, Dr. Puwis Amatyakul, for the advice during this work. Support and assistance from the Geophysics laboratory group members, Mahidol University. I would like to thank Mahidol University for the courtesy of the research facility. I would like to thank my family and friends for their support and to help relieve stress, which is a very important encouragement. Finally, I would like to thank myself for my patience in trying to accomplish this project. Although the COVID-19 situation has had a profound effect on the mental state of work. But even then, it was successful even though the work was less than expected.

Contents

| | |
|--|------------|
| Abstract | i |
| Acknowledgement | ii |
| Table of Contents | iii |
| List of Figures | iv |
| 1 Introduction | 1 |
| 1.1 Aims and Objectives | 1 |
| 1.2 Forward Problem | 1 |
| 1.3 Geophysical Exploration | 2 |
| 2 Background and Related Works | 3 |
| 2.1 Long Offset Transient Electromagnetic (LOTEM) method | 3 |
| 2.2 Basic Theory of Electromagnetic (EM) method | 4 |
| 3 Methodology | 7 |
| 3.1 Project Plan | 7 |
| 3.2 Hankel transform | 7 |
| 3.2.1 Digital Filter | 8 |
| 3.3 Inverse Fourier Transform | 9 |
| 4 Validation and Discussion | 10 |
| 4.1 Analytic Solution for Homogeneous Earth | 10 |
| 4.2 Numerical Solution for Homogeneous Earth | 11 |
| 4.2.1 The magnetic intensity in frequency-domain ($H_z(\omega)$) | 11 |
| 4.2.2 the derivative of vertical magnetic intensity in time-domain $\left(\frac{\partial h_z(t)}{\partial t}\right)$ | 12 |
| 5 Summary | 14 |
| References | 15 |

List of Figures

| | | |
|-----|---|----|
| 1.1 | Forward Modeling | 1 |
| 1.2 | Geophysical Exploration (Burgex Inc., 2017) | 2 |
| 2.1 | LOTEM setup | 3 |
| 3.1 | Project Plan | 7 |
| 3.2 | Hankel Transform | 8 |
| 3.3 | Digital Filter | 9 |
| 4.1 | Analytic Solution of $\frac{dh_z(t)}{dt}$ | 10 |
| 4.2 | LOTEM configuration | 11 |
| 4.3 | The comparison of z in the frequency domain from calculations (right side) and theoretical calculations (left side). | 11 |
| 4.4 | $H_z(\omega)$ by using the summation with weight from (Anderson W.L., 1979). | 12 |
| 4.5 | $\frac{dh_z(t)}{dt}$ from calculations by using the inverse Fourier cosine transform | 12 |
| 4.6 | $\frac{dh_z(t)}{dt}$ calculated from changing the range of ω , the number of ω , the number of time and the range of time | 13 |
| 4.7 | The comparison $\frac{dh_z(t)}{dt}$ from numerical method and analytic method | 13 |

Chapter 1

Introduction

1.1 Aims and Objectives

To develop 1-D forward modeling code of the transient electromagnetic for magnetic field according to ground-dipole source.

1.2 Forward Problem

In the oil industry, they have many drilled holes for sucking oil or injecting water into place instead of the oil. We can know the soil layers from those drilled holes. The oil suction or injecting water may cause the subsurface structure to change. We can see those changes through synthetic data from the forward modeling.

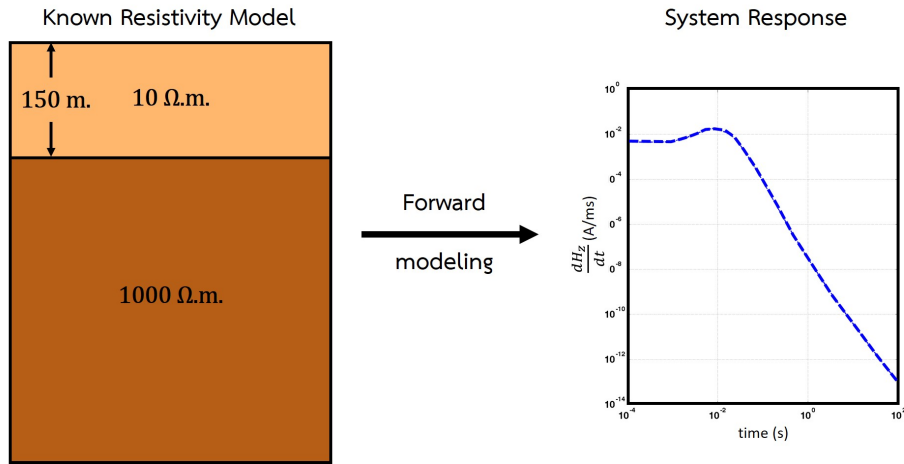


Figure 1.1: Forward Modeling

The picture above shows the process of forward modeling. When we know the model parameter (\mathbf{m}), we can find synthetic data (\mathbf{d}) from the relationship below.

$$\mathbf{d} = A(\mathbf{m})$$

Where A is the forward modeling operator

1.3 Geophysical Exploration

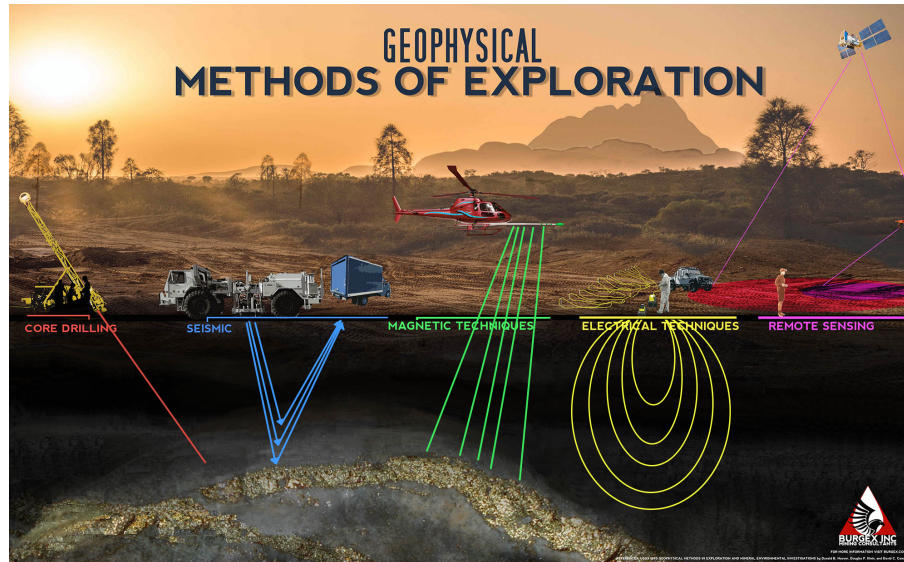


Figure 1.2: Geophysical Exploration (Burgex Inc., 2017)

Geophysics exploration is divided into 5 methods.

1. **Core drilling:** This method has the most accurate results because the rock layer can be seen directly. At the same time, if we want to know the subsurface structure of the wide area, a lot of wells must be dug in order to get the desired results. Digging holes is expensive and may disturb the subsurface structure causing changes.
2. **Seismic:** The reflection seismic represents the evident details of the rock layer under the ground. The refraction seismic represents accurately estimates the depth of each rock layer. But this method does not indicate the difference in the resistance of each type of subsurface structure.
3. **Magnetic Techniques:** Magnetic method is often used for mineral exploration by examining the variations in magnetic mineralogy. The magnetic intensity depends on the magnetization property of the mineral.
4. **Electrical Techniques:** Electrical method is often used for mineral or hydrogeological exploration. This method is divided into several techniques depending on the width of the survey area or the depth to be explored. There will be different tools that are suitable for use in each technique. All techniques use a similar principle to measure the electrical resistivity of the subsurface structure.
5. **Remote Sensing:** The remote sensing method is often used in geoenvironmental to study the differentiation surface with high-resolution images from the near-infrared bands of the electromagnetic spectrum.

In addition to these methods, there are other surveys such as the gravity method. For this project, interested in the electrical method about using the electromagnetic technique called long-offset transient electromagnetic (LOTEM) method.

Chapter 2

Background and Related Works

2.1 Long Offset Transient Electromagnetic (LOTEM) method

The geophysics exploration can be used to find the subsurface structure. In the oil industry, often using the geophysics method that called the long-offset transient electromagnetic (LOTEM) method.

The LOTEM method consists of two parts called the transmitter and the receiver. The distance between the transmitter and the receiver is very far away that they are called offset. The offset is approximately equal to or greater than the exploration depth for the LOTEM method (Strack, 1992). The component of the transmitter is a ground dipole that injects current into the subsurface. The receiver consists of electrodes for measuring electric fields and magnetic fields. The principle of the LOTEM method is when injecting current into the subsurface and conducting current switching. The primary magnetic field occurs, which causes subsequent eddy current in the subsurface. After that, a secondary magnetic field will be formed which is induced by eddy current according to Faraday's law. The current diffuse in the subsurface is related to the conductivity distribution of the subsurface. Then, the receivers measure the voltage difference between the ground in two directions and the vertical magnetic field. The differentiation in the transient curve represent the resistivity contrast of the subsurface structure. The transient time depends on the depth of the structure.

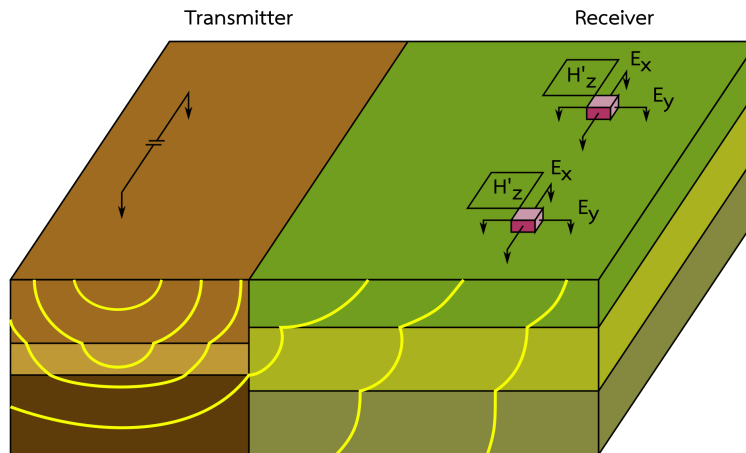


Figure 2.1: LOTEM setup

2.2 Basic Theory of Electromagnetic (EM) method

The initial equation of electromagnetic method is the Maxwell's equations in the time domain (Ward S.H. and Hohmann G.W., 1987).

$$\begin{aligned}\nabla \times \mathbf{E} &= -\frac{\partial \mathbf{B}}{\partial t} \\ \nabla \times \mathbf{H} &= \mathbf{J} + \frac{\partial \mathbf{D}}{\partial t} \\ \nabla \cdot \mathbf{B} &= 0 \\ \nabla \cdot \mathbf{D} &= \rho\end{aligned}$$

and the constitutive relations

$$\begin{aligned}\mathbf{D} &= \epsilon \mathbf{E} \\ \mathbf{B} &= \mu \mathbf{H} \\ \mathbf{J} &= \sigma \mathbf{E}\end{aligned}$$

Where \mathbf{E} is the electric field intensity in (V/m)

\mathbf{B} is the magnetic induction in (Wb/m² or Tesla)

\mathbf{D} is the dielectric displacement in (C/m²)

\mathbf{H} is the magnetic field intensity in (A/m)

\mathbf{J} is the electric current density in (A/m²)

ρ is the electric charge density in (C/m³)

ϵ is the dielectric permittivity in (F/m)

μ is the magnetic permeability in (H/m)

σ is the electric conductivity in (S/m)

We can find wave equations for the electric field and magnetic fields in frequency-domain from the Helmholtz equation.

$$\begin{aligned}\nabla^2 \mathbf{E} + (\mu\epsilon\omega^2 - i\mu\sigma\omega)\mathbf{E} &= 0 \\ \nabla^2 \mathbf{H} + (\mu\epsilon\omega^2 - i\mu\sigma\omega)\mathbf{H} &= 0\end{aligned}$$

The displacement currents are less than the conduction currents ($\mu\epsilon\omega^2 \ll \mu\sigma\omega$) for frequencies less than 10⁵ Hz, so rewritten equations are

$$\begin{aligned}\nabla^2 \mathbf{E} - i\mu\sigma\omega\mathbf{E} &= 0 \\ \nabla^2 \mathbf{H} - i\mu\sigma\omega\mathbf{H} &= 0\end{aligned}$$

Then, continue to perform derivative until the magnetic field components can be written in TE mode and TM mode as expressed as (the derivative is skipped because it's quite long if you are interested, can read more in (Ward S.H. and Hohmann G.W., 1987)):

TM mode

$$\begin{aligned} H_x &= \frac{\partial A_z}{\partial y}, \\ H_y &= -\frac{\partial A_z}{\partial x}, \\ H_z &= 0, \end{aligned}$$

TE mode

$$\begin{aligned} H_x &= \frac{1}{\hat{z}} \frac{\partial^2 F_z}{\partial x \partial z}, \\ H_y &= \frac{1}{\hat{z}} \frac{\partial^2 F_z}{\partial y \partial z}, \\ H_z &= \frac{1}{\hat{z}} \left(\frac{\partial^2}{\partial z^2} + k^2 \right) F_z \end{aligned}$$

Define \mathbf{A} and \mathbf{F}

$$\mathbf{A} = A_z \mathbf{u}_z \quad \text{and} \quad \mathbf{F} = F_z \mathbf{u}_z$$

Where \mathbf{u}_z is a unit vector in z-direction, A_z and F_z are scalar function of x, y, z .

Thus, we can calculate vertical magnetic intensity in the frequency domain due to the finite horizontal electric dipole source by the following equation.

$$\begin{aligned} H_z(\omega) &= \frac{I}{4\pi} \int_{-L}^L \frac{y}{R} \int_0^\infty (1 + r_{TE}) e^{u_0 z} \frac{\lambda^2}{u_0} J_1(\lambda R) d\lambda dx' \\ &= \frac{I(2L)y}{4\pi R} \int_0^\infty (1 + r_{TE}) e^{u_0 z} \frac{\lambda^2}{u_0} J_1(\lambda R) d\lambda \end{aligned}$$

With

$$\begin{aligned} R &= \sqrt{y^2 + L^2} \\ u_0 &= \sqrt{\lambda^2 - i\omega\mu_0\sigma_0} \\ r_{TE} &= \frac{Y_0 - \hat{Y}_1}{Y_0 + \hat{Y}_1} \\ Y_0 &= \frac{u_0}{i\omega\mu_0} \\ \hat{Y}_1 &= Y_1 \frac{\hat{Y}_2 + Y_1 \tanh(u_1 h_1)}{Y_1 + \hat{Y}_2 \tanh(u_1 h_1)} \end{aligned}$$

Where I is the injected current

y is the Tx-Rx distance broadside direction

μ_0 is the magnetic permeability of free space

σ_0 is the conductivity of air

z is the position of Tx in z-axis

λ is the wave number

J_1 is the 1st order Bessel function of the first kind

r_{TE} is the surface reflection coefficient in the TE mode

Y_0 is the intrinsic admittance of the free space

h_i is the thickness of i^{th} layer

L is the distance from center of the dipole to positive or negative electrode

Finally, we can calculate the magnetic versus time by doing the inverse Fourier cosine transform (Newman

G.A., Hohmann G.W. & Anderson W.L., 1986).

$$\begin{aligned}\frac{\partial h_z(t)}{\partial t} &= -\frac{2}{\pi} \int_0^\infty \Re[H_z(\omega)] \cos(\omega t) d\omega \\ h_z(t) &= -\frac{2}{\pi} \int_0^\infty \frac{\Im[H_z(\omega)]}{\omega} \cos(\omega t) d\omega\end{aligned}$$

Chapter 3

Methodology

3.1 Project Plan

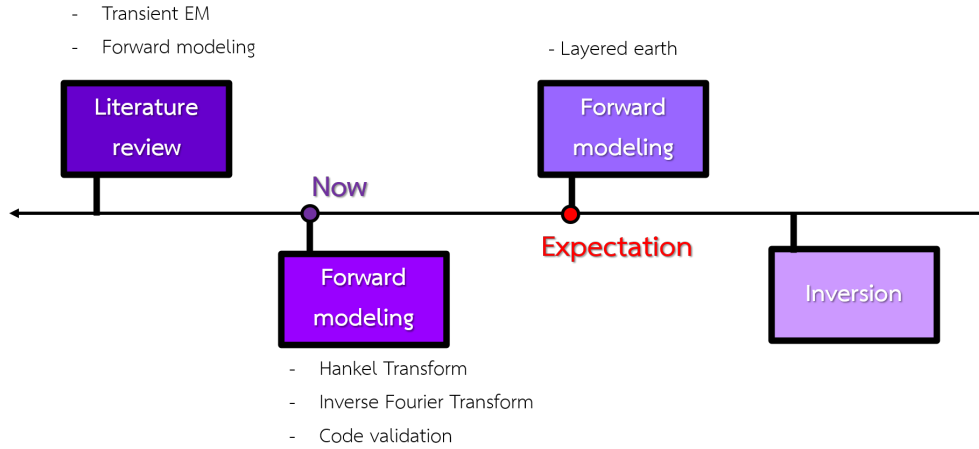


Figure 3.1: Project Plan

The above figure shows the project plan and further work. However, with the COVID-19 situation, causing the work to be delayed and not completed as expected.

3.2 Hankel transform

$$F_v(k) = \int_0^{\infty} f(r) J_v(kr) r dr$$
$$f(r) = \int_0^{\infty} F_v(k) J_v(kr) k dk$$

Where $v \geq \frac{1}{2}$

If we use \int to calculate 0 to ∞ in programming, it will take a long time to calculate and be an endless loop. Therefore, it is necessary to use the summation (\sum) instead of the integral (\int) and specify the range

in the calculation to be suitable for the equation we use.

$$\int_0^\infty r dr \longrightarrow \sum_{i=0}^N r_i$$

The first step is to calculate the Hankel transform by using the functions in MATLAB programs, which are sum, symsum and vpa integral. Assign $F_0(k) = \frac{1}{k}$ which has an analytic solution is $f(r) = \frac{1}{r}$ for the zero-order Bessel function of the first kind.

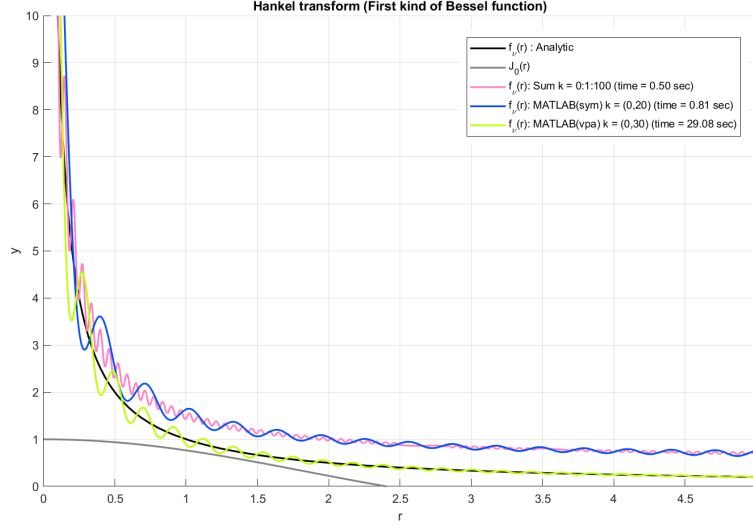


Figure 3.2: Hankel Transform

From the graph, you can see that the results obtained from calculated using various functions in MATLAB also provide results that do not approach the analytic solution and oscillation occurred. Therefore, calculations need to be improved to be more accurate.

3.2.1 Digital Filter

From (Anderson W.L., 1979), we can adjust the numerical integration of the relevant Hankel transform by using the adaptive digital filter as in the equation below.

$$\begin{aligned} K(b) &= \int_0^\infty k(\lambda) J_n(b\lambda) d\lambda \\ &= \frac{\sum_{i=N_1}^{N_2} W_i k[\exp(A_i - x)]}{b}, \quad \text{for } b > 0 \quad \text{and} \quad x = \ln(b) \end{aligned}$$

Where J_n is the Bessel function of the first kind of order n

$k(\lambda)$ is the kernel function

W_i is the filter weight

$A_i - x$ is the shifted abscissa value

The first step is to convert the code from the Fortran program (Anderson W.L., 1979) into the MATLAB

program. Then, using the sample equations below to check the code validity.

$$\int_0^\infty [g \exp(-g^2)] J_0(bg) dg = [\exp(-b^2/4)]/2, \quad (3.1)$$

$$\int_0^\infty [g^2 \exp(-g^2)] J_1(bg) dg = b[\exp(-b^2/4)]/4, \quad (3.2)$$

$$\int_0^\infty [\exp(-g)] J_1(bg) dg = (\sqrt{1+b^2} - 1)/(b\sqrt{1+b^2}), \quad (3.3)$$

$$\int_0^\infty [g \exp(-2g)] J_1(bg) dg = b/(4+b^2)^{3/2}, \quad (3.4)$$

$$\int_0^\infty [\exp(-2g)] J_0(bg) dg = 1/\sqrt{4+b^2} \quad (3.5)$$

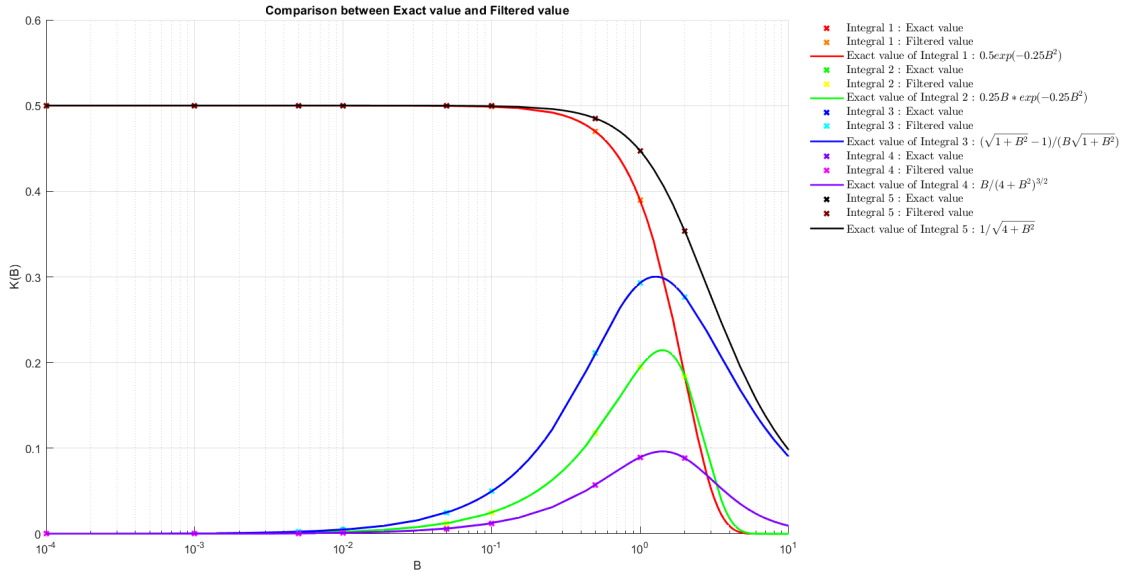


Figure 3.3: Digital Filter

From the code conversion and using the sample equation to verify the accuracy of the code, it is found that the numerical integration of Hankel transform can be precisely calculated with the highest relative error of only 10^{-5} , so the converted code is reliable enough to be adapted to the equations of this project.

3.3 Inverse Fourier Transform

We can convert the frequency-domain to be in the form of the time-domain by using an operator called the inverse Fourier transform, as in the equation below.

$$f(t) = \frac{1}{2\pi} \int_{-\infty}^{\infty} F(\omega) e^{i\omega t} d\omega$$

Where $f(t)$ is the waveform in time-domain

$F(\omega)$ is the waveform in frequency-domain

Chapter 4

Validation and Discussion

4.1 Analytic Solution for Homogeneous Earth

For a homogeneous structure in the earth, an analytic solution can be calculated from the equation below (Ward, S.H. and Hohmann, G.W., 1987).

$$\frac{dh_z(t)}{dt} = \frac{2I}{\pi\mu_0\sigma y^3} \left\{ (1 + \theta^2 y^2) e^{-\theta^2 y^2} \operatorname{erf}(\theta L) - \frac{L}{R} \left(1 + \frac{y^2}{2R^2} \right) \operatorname{erf}(\theta R) + \frac{\theta L y^2}{\sqrt{\pi} R^2} e^{-\theta^2 R^2} \right\}$$

With

$$\begin{aligned}\theta &= \sqrt{\frac{\mu_0\sigma}{4t}} \\ R &= \sqrt{y^2 + L^2}\end{aligned}$$

Where $\operatorname{erf}(\theta)$ is the error function

I is the injected current

y is the Tx-Rx distance broadside direction

μ_0 is the magnetic permeability of free space

σ_0 is the conductivity of air

L is the distance from center of the dipole to positive
or negative electrode

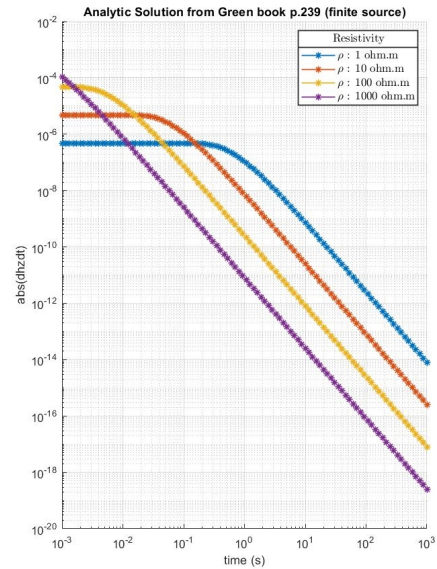


Figure 4.1: Analytic Solution of $\frac{dh_z(t)}{dt}$

4.2 Numerical Solution for Homogeneous Earth

For this project, set the transmitter and receiver in the Cartesian coordinate system at the position (0,0,0) and (0,2000,0) respectively. The injected current is 20 A and the subsurface structure is homogeneous.

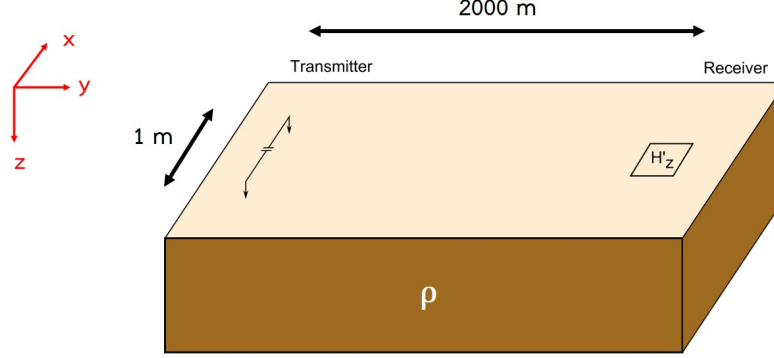
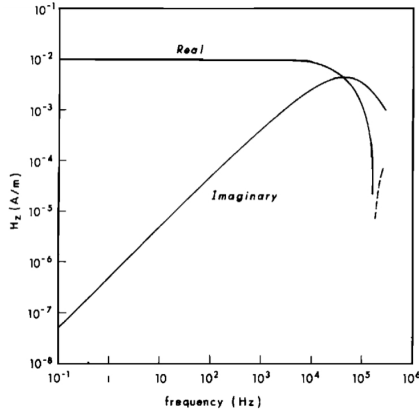
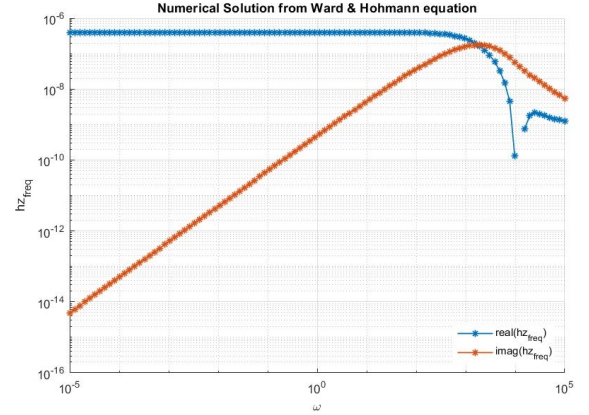


Figure 4.2: LOTEM configuration

4.2.1 The magnetic intensity in frequency-domain ($H_z(\omega)$)



(a) z in the frequency domain that comes from (Ward, S.H. and Hohmann, G.W., 1987).



(b) z in the frequency domain that is calculated using a digital filter from (Anderson W.L., 1979).

Figure 4.3: The comparison of z in the frequency domain from calculations (right side) and theoretical calculations (left side).

From both graphs, you can see that the calculated values of $H_z(\omega)$, both the real and imaginary parts have the same trend as the theoretical values of $H_z(\omega)$ in the book. However, both the calculated value of $H_z(\omega)$ is not equal to the theoretical value, which is caused by the different configurations. Thus, we are able to calculate $H_z(\omega)$ by using a digital filter.

But even then, using the MATLAB coding modified from (Anderson W.L., 1979) takes 48 minutes/100 values of ω . Then, calculated the inverse Fourier transform by assuming to calculate 100 values of the time. It will take 4800 minutes to calculate, or about 4 days, which takes too long.

As the use of the MATLAB coding modified from (Anderson W.L., 1979) takes the time to calculate $H_z(\omega)$ is too long, so try changing the calculations to use summation (\sum) by taking the weight from (Anderson W.L., 1979) multiplying the kernel of the equation that we use, as shown the results in the figure below.

$$\begin{aligned} H_z(\omega) &= \frac{I(2L)y}{4\pi R} \int_0^\infty (1 + r_{TE}) e^{u_0 z} \frac{\lambda^2}{u_0} J_1(\lambda R) d\lambda \\ &= \frac{I(2L)y}{4\pi R} \sum \frac{W_i ((1 + r_{TE}) e^{u_0 z})}{R} \end{aligned}$$

We will see that $H_z(\omega)$ calculated using summation (\sum) is equal to the value obtained from the modified MATLAB coding, and it only takes 2 seconds/100 values of ω , which is faster than 1440 times.

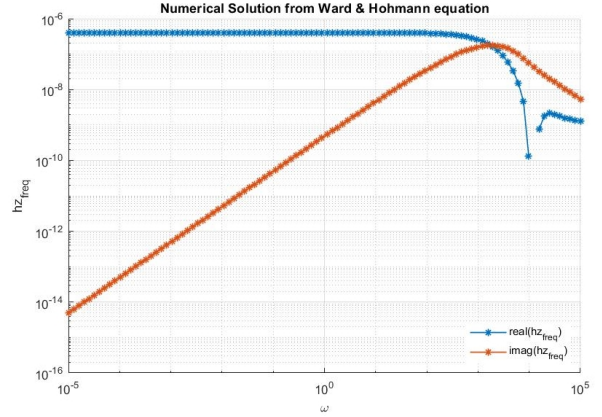


Figure 4.4: $H_z(\omega)$ by using the summation with weight from (Anderson W.L., 1979).

4.2.2 the derivative of vertical magnetic intensity in time-domain $\left(\frac{\partial h_z(t)}{\partial t}\right)$

After the magnetic intensity in frequency-domain ($H_z(\omega)$) are calculated and then can be calculated the derivative of vertical magnetic intensity in time-domain $\left(\frac{\partial h_z(t)}{\partial t}\right)$ by using the inverse Fourier cosine transform.

$$\frac{\partial h_z(t)}{\partial t} = -\frac{2}{\pi} \int_0^\infty \Re[H_z(\omega)] \cos(\omega t) d\omega$$

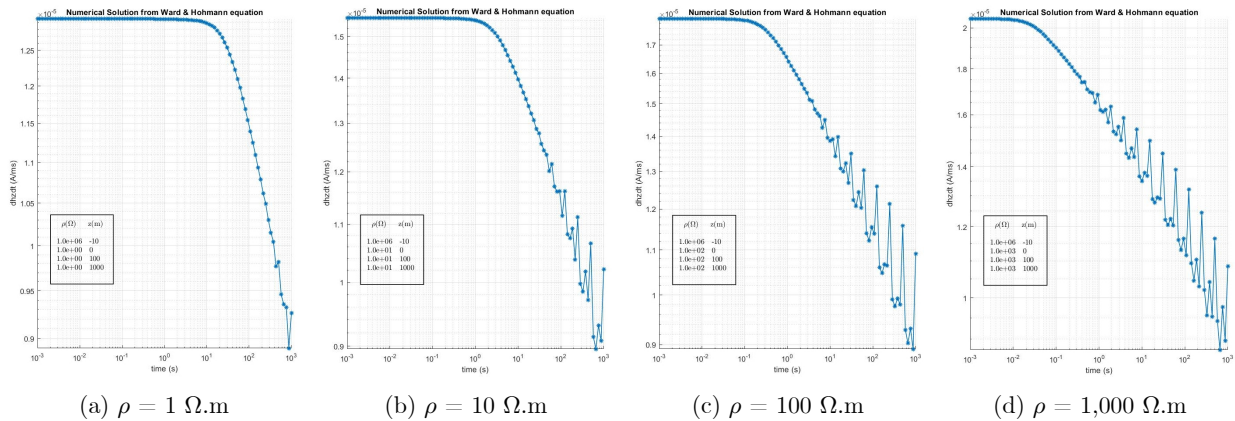


Figure 4.5: $\frac{dh_z(t)}{dt}$ from calculations by using the inverse Fourier cosine transform

All figures above show that oscillations occur at large intervals (low ω values) and wider oscillations when the structure has a high resistivity structure.

Thus, adjust the range of ω , number of ω , number of time and range of time until the optimal range for calculation is $\omega = \text{logspace}(-8, 4, 200)$ and time = $\text{logspace}(3, 3, 100)$, which is shown in the figures below.

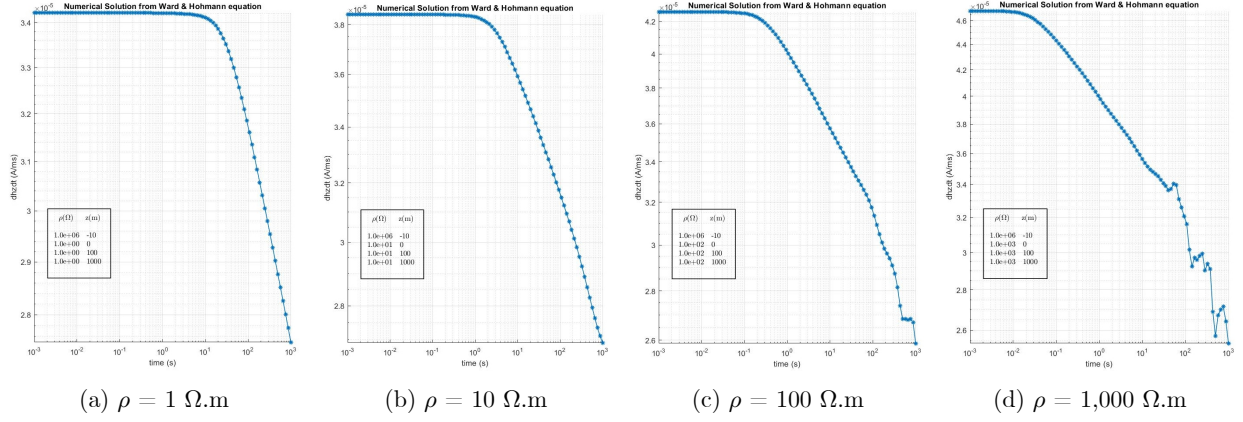


Figure 4.6: $\frac{dh_z(t)}{dt}$ calculated from changing the range of ω , the number of ω , the number of time and the range of time

It is evident that the oscillation reduced to almost none in the resistivity structure (ρ) = 1 and 10 $\Omega.m$ but for resistivity structure (ρ) = 100 and 1,000 $\Omega.m$ also the oscillation occurs at time > 10 second.

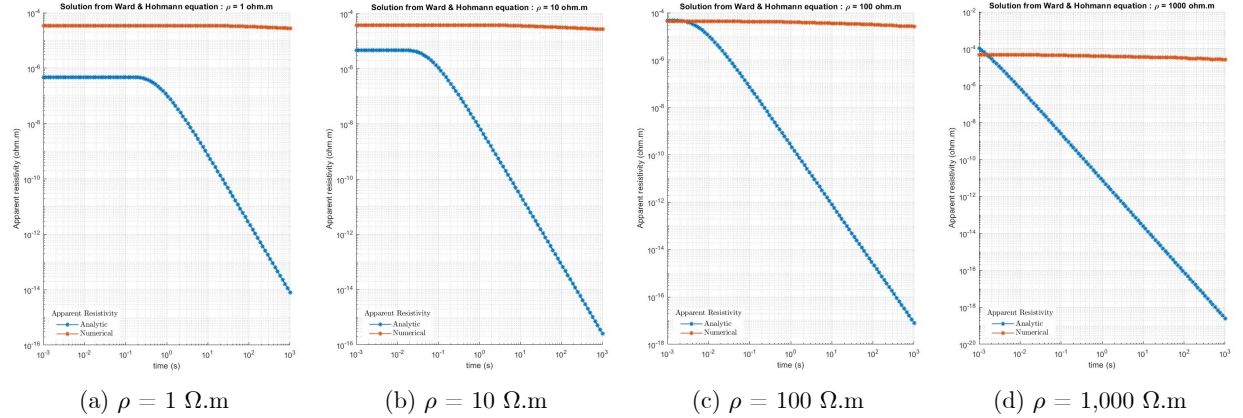


Figure 4.7: The comparison $\frac{dh_z(t)}{dt}$ from numerical method and analytic method

When comparing the values of $\frac{\partial h_z(t)}{\partial t}$ compared with the numerical solution and the analytic solution, it appears that the trend is the same. But even then, the value of $\frac{\partial h_z(t)}{\partial t}$ that is calculated by numerical method changes too small compared to the analytic solution, so it is almost seen as a straight line.

Therefore, we need to find a method to solve it by multiplying the weight from optimization during calculated the inverse Fourier cosine transform, so the expected results maybe even better.

Chapter 5

Summary

This project involves the forward modeling of the geophysics method, which is called a long-offset transient electromagnetic (LOTEM) method. The objective is to compare the subsurface structure from calculated the derivative of vertical magnetic intensity measured from air-loop and the vertical magnetic intensity measured by the fluxgate magnetometer. The calculation starts from Maxwell's equations and constitutive equations. Then, find the TE mode and TM mode of the magnetic field until finally get the magnetic intensity in frequency-domain ($H_z(\omega)$). After that, it can find the derivative of vertical magnetic intensity $\left(\frac{dh_z(t)}{dt}\right)$ and the vertical magnetic intensity ($h_z(t)$) obtained from inverse the Fourier cosine transform. To verify the accuracy of the calculation, compare the numerical solution of the derivative of vertical magnetic intensity $\left(\frac{dh_z(t)}{dt}\right)$ of homogeneous structure with theoretical analytic solutions (Ward, SH and Hohmann, GW, 1987). First, calculate the numerical integration of magnetic intensity in frequency-domain ($H_z(\omega)$). It was found that applying a digital filter from (Anderson W.L., 1979) in the integration of Hankel transforms to get a suitable value. Then, calculate the inverse Fourier cosine transforms. In the beginning, it was found that the oscillations occur at large intervals (low ω values) and wider oscillations when the structure has a high resistivity structure. Then adjust the range of ω , number of ω , number of time and range of time until the optimal range for calculation is $\omega = \text{logspace}(-8, 4, 200)$ and $\text{time} = \text{logspace}(3, 3, 100)$. But even so, the oscillation occurs at $\text{time} > 10$ second for resistivity structure (ρ) = 100 and 1,000 $\Omega.m$. Finally, compare the values of $\frac{\partial h_z(t)}{\partial t}$ between the numerical solution and the analytic solution, it appears that the trend is the same. But even then, the value of $\frac{\partial h_z(t)}{\partial t}$ that is calculated by numerical method changes too small compared to the analytic solution, so it is almost seen as a straight line.

Therefore, we need to find a method to solve it by multiplying the weight from optimization during calculated the inverse Fourier cosine transform, so the expected results maybe even better.

References

- [1] Anderson, W.L. 1979, Computer Program Numerical integration of related Hankel transforms of orders 0 and 1 by adaptive digital filtering, In: *Geophysics*, 44, 1287-1305.
- [2] Christiansen, A.V., Auken, E., Sørensen, K., 2009, The transient electromagnetic method, In: *Ground-water geophysics*, pp. 179-266., Springer Berlin Heidelberg
- [3] Newman, G. A., Hohmann, G. W. & Anderson, W. L., 1986. Transient electromagnetic response of a three-dimensional body in a layered-earth, *Geophysics*, 51, 1608-1627.
- [4] Rochlitz, R., Queitsch, M., Yogeshwar, P., Günther, T., Chwala, A., Janser, S., Kukowski, S., Stolz, R., 2018, Capability of low-temperature SQUID for transient electromagnetics under anthropogenic noise conditions, In: *Geophysics*, 2018, 83, 6
- [5] Strack, K.M., 1992, *Exploration with deep transient electromagnetics*. Elsevier, 373 pp.
- [6] Ward, S.H. and Hohmann, G.W. 1987. Electromagnetic theory for geophysical applications. In: Investigations in *Geophysics 3: Electromagnetic Methods in Applied Geophysics* (ed. M.N. Nabighian), pp. 131–311., Society of Exploration Geophysicists.